2.B:2.G

Nuclear Physics A228 (1974) 216—228;

THE (d, ^{6}Li) REACTION IN THE f-p SHELL AT E_d = 27.25 MeV

A. E. CEBALLOS, H. J. ERRAMUSPE †, A. M. J. FERRERO, M. J. SAMETBAND †
J. E. TESTONI †, D. R. BÈS †, E. E. MAQUEDA †, R. P. J. PERAZZO † and S. L. REICH
Comisión Nacional de Energía Atómica, Departamento de Física Nuclear,
Av. Libertador 8250, Buenos Aires (29), Argentina

Received 8 April 1974

Abstract: The differential cross sections for the reactions ^{56}Fe(d, ^{6}Li)^{52}Cr and ^{58}Ni(d, ^{6}Li)^{54}Fe leading to the ground 0^+ and the first 2^+ excited states are measured at 27.25 MeV. A DWBA analisis of these data and those previously obtained for three Zn isotopes at the same energy is performed. The calculation of the microscopic form factors is carried out within the framework of different approximations.

E NUCLEAR REACTIONS ^{56}Fe(d, ^{6}Li)^{52}Cr, ^{58}Ni(d, ^{6}Li)^{54}Fe, E = 27.25 MeV; measured $\sigma(\theta)$. ^{52}Cr and ^{54}Fe levels deduced relative S. Enriched targets.

1. Introduction

In a recent paper [1]) (d, ^{6}Li) reactions at E_d = 27.25 MeV induced on ^{64,66,68}Zn isotopes were reported and the experimental results analyzed using both phenomenological and microscopic form factors. The microscopic form factors were calculated on the basis of a BCS plus RPA description of the initial states and the first 0^+ and 2^+ states of the residual nuclei. Here, we extend the experimental differential cross-section data by including the (d, ^{6}Li) reactions on ^{56}Fe and ^{58}Ni targets and make an overall discussion of (d, ^{6}Li) reactions in the f-p shell using different approaches to the microscopic description of the nuclear states.

In sect. 2 we describe the experimental procedure. In sect. 3 we show the experimental data and make a DWBA analysis of the differential cross sections. Sect. 4 is devoted to the microscopic calculations of the form factors which are carried out in four different ways: (i) through an exact diagonalization of the residual pairing force in a four-level shell model basis; (ii) considering a simple shell model configuration to account for the cross sections leading both to the 0^+ and the first 2^+ excited states of the ^{52}Cr and ^{56}Fe residual nuclei; (iii) assuming that the (d, ^{6}Li) reaction leading to the 0^+ ground states of the final nuclei are transitions between vibrational states of the $T = 1$ pairing Hamiltonian with ^{56}Ni as the zero-phonon state; (iv) by a BCS treatment of the pairing degree of freedom in the Zn region.

Finally in sect. 5 we make a general discussion of the results on four-particle transfer reactions in the f-p shell in the light of the different approaches.

† Fellow of the Consejo Nacional de Investigaciones Científicas y Técnicas.

2. Experimental method

The measurements described in this paper have been performed by bombarding self-supporting metallic foils of ^{56}Fe and ^{58}Ni with the 27.25 MeV deuteron beam of the Buenos Aires 180 cm synchrocyclotron.

The experimental set-up was similar to that reported in ref. [1]). Considerations about the Q-values and stopping power for the different possible products of the reaction allowed a good identification of the ^{6}Li ions for the first 0^+ and 2^+ states of the residual nuclei by using E-ΔE telescopes of (100-50)μm and (90-50)μm fully depleted surface barrier Si detectors.

Nevertheless in the case of ^{56}Fe this situation was modified by the presence of the ^{6}Li ions produced in the ^{16}O(d, ^{6}Li)^{12}C reaction. The cross section for this reaction was measured by bombarding a PbO target and the yields were subtracted from the corresponding ones in ^{56}Fe(d, ^{6}Li)^{52}Cr. Unfortunately, the poor statistics obtained and the overlap with the 2^+ level of ^{52}Cr did not permit a correct evaluation of the angular distribution at forward angles.

The overall energy resolution obtained was 400 keV FWHM.

The targets used in the experiment were enriched self-supporting foils of ^{56}Fe (99.95 %) and ^{58}Ni (99.96 %), 0.800 mg · cm^{-2} and 1.13 mg · cm^{-2} thick respectively.

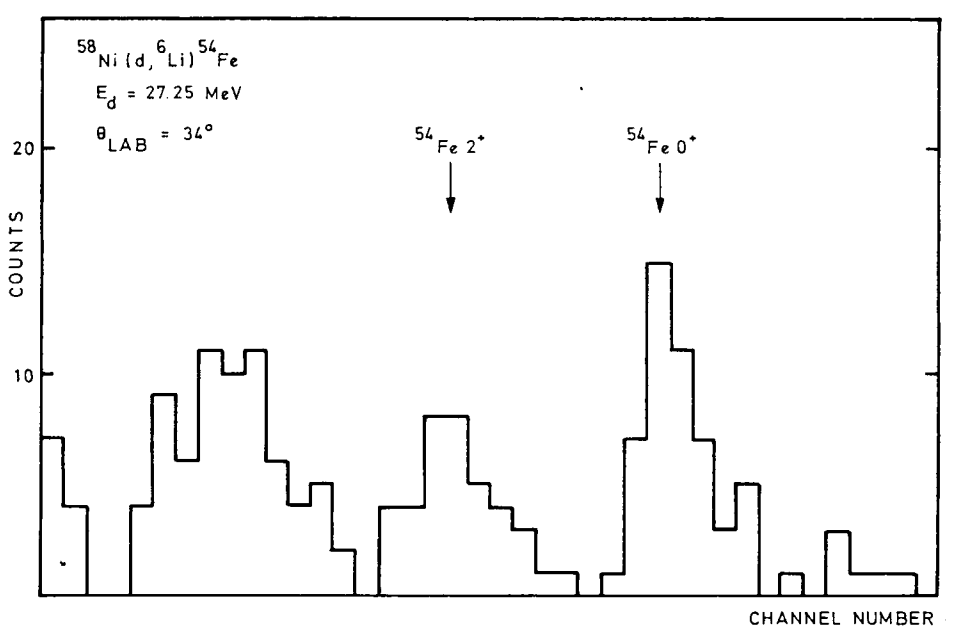

Fig. 1. The spectrum of Li ions obtained in reactions on ^{58}Ni induced by 27.25 MeV deuterons, at $\theta_{lab} = 34°$.

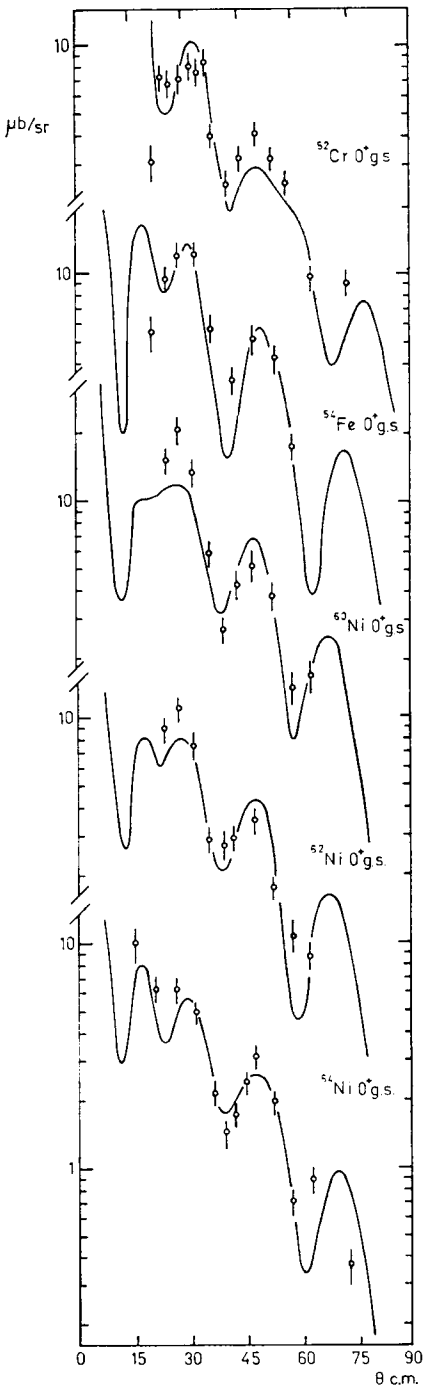

Fig. 2. The differential cross sections of the reactions ^{56}Fe(d, ^{6}Li)^{52}Cr, ^{58}Ni(d, ^{6}Li)^{54}Fe and ^{64,66,68}Zn(d, ^{6}Li)^{60,62,64}Ni, leading to the 0^+ ground state at $E_d = 27.25$ MeV. Solid lines represent the DWBA calculations.

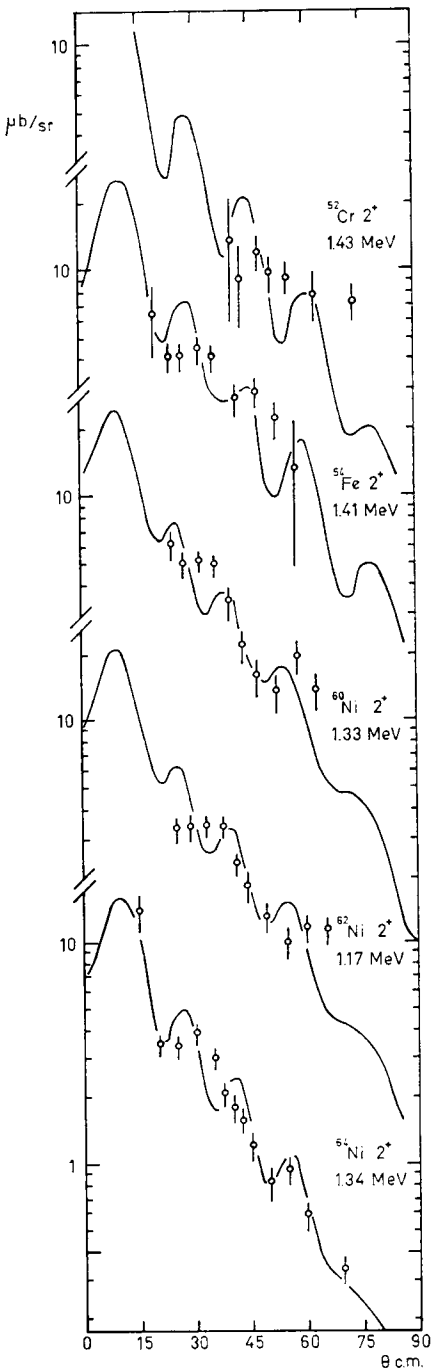

Fig. 3. The differential cross sections of the reactions ^{56}Fe(d, ^{6}Li)^{52}Cr, ^{58}Ni(d, ^{6}Li)^{54}Fe and ^{6},^{66,68}Zn(d, ^{6}Li)^{60,62,64}Ni, leading to the 2^+ first excited state at $E_d = 27.25$ MeV. Solid lines represent the DWBA calculations.

3. Experimental results and DWBA analysis

Fig. 1 shows the spectrum of the ^{6}Li ions produced in the ^{58}Ni(d, ^{6}Li)^{54}Fe reaction at 34° in the lab system. Only the 0^+ ground state and 1.409 MeV 2^+ level of the residual nucleus are resolved; the ^{53}Fe states populated in the ^{58}Ni(d, ^{7}Li)^{53}Fe reaction are at least 11.30 MeV below the 0^+ ground state of ^{54}Fe. Given the Q-values for the (d, ^{6}Li) reactions this situation is observed in all the spectra belonging to nuclei of the medium mass region.

Figs. 2 and 3 show the differential cross sections corresponding to the reactions ^{56}Fe(d, ^{6}Li)^{52}Cr and ^{58}Ni(d, ^{6}Li)^{54}Fe leading to the 0^+ states and the first 2^+ excited states at 1.433 MeV and 1.409 MeV respectively. To account for the calculations of sect. 4 the differential cross sections reported in ref. [1]) are also plotted. The data are given in the c.m. system.

The patterns and magnitudes of the angular distributions in the zone close to the doubly magic nucleus ^{56}Ni are quite similar to those obtained in the Zn region. This fact suggests the pick-up of a superficial α-cluster through a mechanism independent of the progressive filling of the shell. The absolute magnitudes of the cross sections range from 1 μb/sr to 20 μb/sr.

The DWBA analysis was carried out with the code DWUCK [2]) under the hypothesis of a direct reaction and formulating the same assumptions as in sect. 4 of ref. [1]). To get a good agreement between the experimental data and the computed cross sections in the Ni region it was only necessary to change slightly the V-values for the real optical well used in the Zn region. The optical parameters are shown in table 1.

The form factor has been constructed by the addition of coherent contributions

TABLE 1

The optical parameters for the deutron and lithium channels and the parameters for the bound α-particle well

	d-channel	Li channel	α-particle well
V (MeV)	71.9	310 for ^{56}Fe 312 for ^{58}Ni 328 for ^{64}Zn 321 for ^{66}Zn 310 for ^{68}Zn	adjusted to get the binding energy
W (MeV)	56.0	75.0	
r_{0V} (fm)	0.96	1.50	1.25
a_V (fm)	0.99	0.65	0.65
r_{0W} (fm)	1.35	1.50	
a_W (fm)	0.75	0.65	
r_{0c} (fm)	1.25	2.50	1.25
a_c (fm)	0.00	0.00	0.00

TABLE 2
The renormalization factors D_0^2 for the different models

	0^+				2^+	
	shell model	harmonic model	pure configs.	BCS	shell model	BCS
^{56}Fe	23 ±6	20 ±5	330±50		160±60	
^{58}Ni	28 ±3	41 ±4	550±50		255±55	
^{64}Zn	11 ±4	7.2±3.0		20±7		48±6
^{66}Zn	9.5±2.0	4.1±1.0		17±4		39±7
^{68}Zn	12 ±1	3.4±0.3		24±1		36±4

corresponding to the allowed orbital quantum numbers N for the configurations included in the calculations of the structure factor G_{NL} as is discussed in sect. 4. The potential depth in which the transferred α-particle is bound is adjusted to obtain the correct binding energies.

Solid lines in figs. 2 and 3 correspond to the DWBA calculations computed with the G_{NL} factors obtained in the four-level and the single configuration shell model and BCS approaches respectively, as described in sect. 4. Each curve is normalized with the corresponding value of $D_0^2 = \sigma_{\text{exp}}/\sigma_{\text{DWUCK}}$ (see table 2). The shapes of the differential cross sections for the different approximations are essentially the same.

4. Microscopic construction of the form factor

4.1. TRANSITIONS POPULATING THE $J^\pi = 0^+$ STATES

The analysis of the α-transitions populating $J^\pi = 0^+$ states has been made under the assumption that the main component of the residual nuclear interaction which is relevant for this process is the $T = 1$ part of the pairing force†. We perform an exact shell model diagonalization of this force within the f-p shell, and we compare the results with those that have been obtained with some extra simplifying assumptions (pure configurations, harmonic description, BCS). Consequently, as a result of our analysis, we may make conclusions about:

(i) The importance of the $T = 0$ component of the pairing force. This could be done by comparing the agreement between theoretical and empirical spectroscopic factors for both small and relatively large values of T.

(ii) The validity of the simphfying assumptions, from the comparison with the exact shell model diagonalization.

4.1.1. Exact diagonalization of the pairing force. The diagonalization of the pairing force with $T = 1$ proceeds along the same lines as in refs. [3,4]) and, therefore, technical details are omitted here. Two major differences with respect to the calculation

† This is similar to the approximation that is usually made in connection with α-emission in heavy nuclei.

of ref. [4]) are introduced. In the first place, the four f-p single-particle levels are included here and, secondly, a truncation of the shell model space is performed in order to carry out the diagonalization.

The four parameters involved in the calculation are the three distances between the single-particle levels and the strength of the pairing force G. The energy differences between the $f_{\frac{7}{2}}$, $p_{\frac{3}{2}}$ and $f_{\frac{5}{2}}$ levels are fixed at the same values as in ref. [4]). The presence of the $p_{\frac{1}{2}}$ single-particle state gives rise to another non-adiabatic (incoherent) addition mode. Two $J^\pi = 0^+$ states at about 6.5 MeV are populated in the reactions ^{58}Ni(t, p)^{60}Ni and ^{58}Ni(τ, n)^{60}Zn, respectively, with appreciable intensity. We have assumed that these states can be described in terms of the non-adiabatic pairing mode involving mainly the creation of two particles in the $(p_{\frac{1}{2}})^2$ state. The position of the corresponding 0^+ states is very sensitive to the distance between the $p_{\frac{1}{2}}$ and $p_{\frac{3}{2}}$ levels, which is taken to be 2.30 MeV†.

On the other hand, the properties of the 6.58 MeV state in ^{56}Ni are not very sensitive to the presence of the $p_{\frac{1}{2}}$ single-particle state, but they are rather due to the fact that the inclusion of this level requires a different renormalization of the pairing force strength. In order to obtain the energy for this state as in ref. [4]), where the $p_{\frac{1}{2}}$ level was excluded, we must decrease the strength of the pairing force from $30/A$ MeV to $25/A$ MeV.

Concerning the truncation of the shell model space, we allow up to four particle-hole pairs on top of the zeroth-order configuration corresponding to each ground state. For the case of ^{56}Ni we have verified that this is indeed a good approximation by comparing with a diagonalization performed in the complete f-p space. In this case the sum of the squares of the amplitudes corresponding to the components ignored in the truncated spaces is $\lesssim 2\,\%$.

The relevant spectroscopic information for the reaction calculation is obtained from the matrix element

$$C(jj'01) = \frac{1}{2\sqrt{2T+1}} \langle \psi_i^T(A) || \{\beta_j^+ \beta_{j'}^+\}^{t=0} || \psi_f^T(A-4) \rangle, \tag{1}$$

where

$$\beta_j^+ = \{b_j^+ b_j^+\}^{I=0,t=1}. \tag{2}$$

The spectroscopic amplitudes (1) are used as in ref. [5]) in order to calculate the G_{NL} factors, which measure the overlap between the α-particle and the wave function of the picked-up nucleons in the $A+4$ system. Other amplitudes $C(jj'J_2T_2)$, with $J_2 \neq 0$ or/and $T_2 \neq 1$ contribute to build the G_{NL} according to a chain-of-two-particles fractional parentage technique used in ref. [5]), but they can be obtained from (1) by means of the overlap of the four-particle wave functions.

4.1.2. Pure configurations. When dealing with transitions to the 2^+ final excited

† This interpretation of the 6.4 MeV state in ^{60}Ni and 6.9 MeV state in ^{60}Zn has been confirmed through a DWBA analysis of the two-particle transition strength, although the predicted cross section appears to be somewhat larger than the experimental value.

states (see subsect. 4.2) an exact diagonalization will be no longer possible and only approximate treatments will be made. In order to have a comparable treatment for one of those approximations, also the ground 0^+ states are calculated assuming a pure configuration. In particular, this is done for the transitions ^{58}Ni(d, ^{6}Li)^{54}Fe and ^{56}Fe(d, ^{6}Li)^{52}Cr where the following configurations are assumed

$$|^{58}\mathrm{Ni}, J = 0\rangle \equiv |(\mathrm{f}_{\frac{7}{2}})_{\mathrm{p}}^{8}(\mathrm{p}_{\frac{3}{2}})_{\mathrm{n}}^{2}, J = 0\rangle, \tag{3a}$$

$$|^{56}\mathrm{Fe}, J = 0\rangle \equiv |(\mathrm{f}_{\frac{7}{2}})_{\mathrm{p}}^{6}(\mathrm{p}_{\frac{3}{2}})_{\mathrm{n}}^{2}, J = 0\rangle, \tag{3b}$$

$$|^{54}\mathrm{Fe}, J\rangle \equiv |(\mathrm{f}_{\frac{7}{2}})_{\mathrm{p}}^{6}, J\rangle, \tag{3c}$$

$$|^{52}\mathrm{Cr}, J\rangle \equiv |(\mathrm{f}_{\frac{7}{2}})_{\mathrm{p}}^{4}, J\rangle. \tag{3d}$$

4.1.3. Harmonic description. The description of the initial and final states in terms of the removal (r) and addition (a) phonons is made as in refs. [6,7]). In the phonon basis, the operators β_j^+ of eq. (2) are written in terms of creation and annihilation phonon operators:

$$\beta_j^+ = \begin{cases} \lambda_j^{(\mathrm{a})}\Gamma_{\mathrm{a}}^+ + \mu_j^{(\mathrm{r})}\Gamma_{\mathrm{r}}^+ & j = \mathrm{p}_{\frac{3}{2}}, \mathrm{f}_{\frac{5}{2}}, \mathrm{p}_{\frac{1}{2}} \\ \mu_j^{(\mathrm{a})}\Gamma_{\mathrm{a}}^+ + \lambda_j^{(\mathrm{r})}\Gamma_{\mathrm{r}}^+ & j = \mathrm{f}_{\frac{7}{2}}. \end{cases} \tag{4}$$

The determination of the coefficients λ and μ is made by equalizing them to the matrix elements that were obtained in the previous shell model diagonalization:

$$\begin{aligned} \langle ^{58}\mathrm{Ni}, \text{g.s.}||\beta_j^+||^{56}\mathrm{Ni}, \text{g.s.}\rangle &= \langle \Gamma_{\mathrm{a}}^+||\beta_j^+||0\rangle = \begin{cases} \sqrt{3}\lambda_j & j = \mathrm{p}_{\frac{3}{2}}, \mathrm{f}_{\frac{5}{2}}, \mathrm{p}_{\frac{1}{2}} \\ \sqrt{3}\mu_j & j = \mathrm{f}_{\frac{7}{2}}, \end{cases} \\ \langle ^{56}\mathrm{Ni}, \text{g.s.}||\beta_j^+||^{54}\mathrm{Fe}, \text{g.s.}\rangle &= \langle 0||\beta_j^+||\Gamma_{\mathrm{r}}^+\rangle = \begin{cases} -\sqrt{3}\mu_j & j = \mathrm{p}_{\frac{3}{2}}, \mathrm{f}_{\frac{5}{2}}, \mathrm{p}_{\frac{1}{2}} \\ -\sqrt{3}\lambda_j & j = \mathrm{f}_{\frac{7}{2}}. \end{cases} \end{aligned} \tag{5}$$

Introducing (4) in (1) we obtain the spectroscopic amplitudes $C(jj'01)$ after some recoupling algebra and using the reduced matrix elements [3]) $\langle n \pm 1, t \pm 1||\Gamma^+||n, t\rangle$.

The ^{58}Ni and ^{54}Fe ground states are pictured as an addition and a removal phonon, respectively, while the ^{56}Fe ground state is made up by an addition and a removal phonon coupled to $T = 2$, and the ^{52}Cr ground state as two removal phonons coupled to $T = 2$. Therefore, for both the ^{58}Ni(d, ^{6}Li)^{54}Fe and ^{56}Fe(d, ^{6}Li)^{52}Cr reactions, the spectroscopic amplitudes are proportional to the matrix elements of the operators $\{\Gamma_{\mathrm{r}}^+\Gamma_{\mathrm{a}}\}^{t=0}$:

$$\begin{aligned} \frac{C(jj', {}^{58}\mathrm{Ni} \to {}^{54}\mathrm{Fe})}{C(jj', {}^{56}\mathrm{Fe} \to {}^{52}\mathrm{Cr})} &= \sqrt{\frac{5}{3}}\, \frac{\langle \Gamma_{\mathrm{r}}^+||\{\Gamma_{\mathrm{r}}^+\Gamma_{\mathrm{a}}\}^0||\Gamma_{\mathrm{a}}^+\rangle}{\langle \{\Gamma_{\mathrm{r}}^+\Gamma_{\mathrm{r}}\}^2||\{\Gamma_{\mathrm{r}}^+\Gamma_{\mathrm{a}}\}^0||\{\Gamma_{\mathrm{r}}^+\Gamma_{\mathrm{a}}^+\}^2\rangle} \\ &= \sqrt{\tfrac{1}{2}}. \end{aligned} \tag{6}$$

The ratio of the transitions corresponding to the ^{56}Fe and ^{58}Ni targets is expected to be about two and similar to the pure configurations case (aside from Pauli corrections), although their absolute value should be considerably larger.

4.1.4. Superconducting solution. The collective treatment of the pairing degree of

freedom allows one to proceed further than the harmonic description and, eventually, to reach the limit in which a permanent distortion appears. In this other extreme case [6-8]), the degrees of freedom are represented by rotations in isospace and gauge space plus vibrations around the equilibrium positions. The last ones are determined by two deformation parameters, Δ_n and Δ_p, corresponding to the neutron and proton superconducting gaps in the intrinsic frame or, alternatively, by the related parameters

$$\Delta = \{\Delta_n^2 + \Delta_p^2\}^{\frac{1}{2}}, \qquad \Gamma = \mathrm{tg}^{-1}\left(\frac{\Delta_n - \Delta_p}{\Delta_n + \Delta_p}\right). \tag{7}$$

The ground state of single closed shell nuclei (such as ^{A}Ni isotopes with $A > 58$) may be described in terms of the yrast approximation [9,10]) corresponding to $\Gamma_{eq} = \frac{1}{4}\pi$ or $\Delta_n = \Delta$, $\Delta_p = 0$. Thus, only the (intrinsic) neutrons become superconductors and the set of ground states constitutes the yrast band.

The effect of two protons in the ground state of Zn isotopes can be described in terms of one-phonon excitations of an oscillator in the Δ_p coordinate (Γ-vibrations). In this approximation (1) is given as a product of two processes, namely the de-excitation of a Γ-vibration and the (stronger) transition between two consecutive members of an yrast band. We simulate this calculation via the exact shell model diagonalization by introducing in (1) only two intermediate states corresponding to the ground states of the $^{A-2}$Zn and $^{A-2}$Ni isotopes respectively (for the transition from ^{A}Zn to $^{A-4}$Ni).

The previous microscopic calculation corresponding to the yrast description can be done in a simpler way [1]) by describing the neutrons, in both the Zn and Ni isotopes, by means of the usual BCS solution. In the Zn isotopes, the two last protons move like valence particles in the shell starting at $Z = 28$ protons†. The operator corresponding to the α-particle transfer between 0^+ states is

$$T_0^+ = \frac{1}{\sqrt{3}}\left(1 + \frac{2j+3}{2j+1}\delta_{jj'}\right)(b_j^+ b_j^+)_1^{01}(b_{j'}^+ b_{j'}^+)_{-1}^{01}, \tag{8}$$

with matrix elements

$$\langle {}^{A-4}\mathrm{Ni}, \text{g.s.}|T_0|{}^A\mathrm{Zn}, \text{g.s.}\rangle = \sqrt{\tfrac{2}{3}}\lambda_{j'}\left(1 + \frac{2j+3}{2j+1}\delta_{jj'}\right) \times (-)^j\sqrt{2j+1}\,U_j V_j. \tag{9}$$

In the above expression $\lambda_{j'}$ are the amplitudes of the $|(j')^2\rangle$ components in the two-proton wave function. They are obtained assuming a pairing interaction with strength $G_p = 0.714$ MeV, resulting in $\lambda_{\frac{3}{2}} = 0.68$, $\lambda_{\frac{7}{2}} = 0.71$ and $\lambda_{\frac{1}{2}} = 0.19$. The BCS parameters U_j and V_j are obtained by solving the number and gap equations for the seven neutron orbitals starting with $f_{\frac{7}{2}}$.

The value of the pairing strength was $G_n = 0.346$ MeV and the single-particle levels energies are those of table 3 in ref. [1]).

† This model was applied in ref. [1]). However, there is a mistake in the matrix elements obtained there. Because of this we give the formulae here explicitly.

4.2. ANALYSIS OF TRANSITIONS POPULATING $J^\pi = 2^+$ STATES

As stated already, in this case it is more difficult to perform a complete shell model diagonalization. However, because of the reasonable agreement which was found for $J^\pi = 0^+$ states between the exact diagonalization of the pairing force and simpler treatments of the same interaction, we may attempt to apply also here some simplifying assumptions.

We divide the experimental material in two groups of transitions, according to whether they take place around $A = 56$ or on Zn targets. For the first group it is easy to perform a calculation with almost pure configurations. As in the previous case we expect that the corresponding results should significantly underpredict the absolute cross sections, but we expect better relative cross sections.

The corresponding configurations were given in eqs. (3a–3d). For 2^+ final state in ^{52}Cr, there are two states corresponding to four particles (or four holes) in the $f_{\frac{7}{2}}$ shell, coupled to $J = 2$. A possible choice of two orthogonal states would be

$$|1\rangle = |\{(b^+_{\frac{7}{2}} b^+_{\frac{7}{2}})^{01}(b^+_{\frac{7}{2}} b^+_{\frac{7}{2}})^{21}\}^{22}\rangle,$$

$$|2\rangle = -0.804|\{(b^+_{\frac{7}{2}} b^+_{\frac{7}{2}})^{01}(b^+_{\frac{7}{2}} b^+_{\frac{7}{2}})^{21}\}^{22}\rangle + 1.283|\{(b^+_{\frac{7}{2}} b^+_{\frac{7}{2}})^{21}(b^+_{\frac{7}{2}} b^+_{\frac{7}{2}})^{21}\}^{22}\rangle, \quad (10)$$

where the kets are properly normalized. The lower 2^+ states in ^{52}Cr are a linear combination of these states,

$$|^{52}\mathrm{Cr}, J = 2\rangle = \alpha|1\rangle + \beta|2\rangle. \quad (11)$$

The transition spectroscopic amplitude C is then obtained in terms of the coefficients α and β. In order to get maximum coherence for the $0^+ \to 2^+$, E2 transition in ^{52}Cr, the sign of β must be chosen opposite to that of α. Under this assumption the values of the amplitude C are restricted to a very narrow interval which can be further confined if the lower state is assumed to have a large seniority-2 component. The α-values used in this calculation are not far from unity as it is suggested by the fact that the pairing force is diagonal in the basis $|1\rangle$ and $|2\rangle$.

In the case of the ^{A}Zn targets, the final $J^\pi = 2^+$ states of the $^{A-4}$Ni isotopes are described in terms of the pairing-plus-quadrupole model, which are treated within the BCS and RPA approximations [11,12]). Here the T^+_{20} four-body operator is

$$T^+_{20}(j_1\, j_2\, j_3\, j_3) = F(j_1\, j_2\, j_3)(b^+_{j_1} b^+_{j_2})^{21}_{01}(b^+_{j_3} b^+_{j_3})^{01}_{0-1}, \quad (12)$$

where

$$F(j_1\, j_2\, j_3) = \begin{cases} \sqrt{\frac{1}{3}} & \text{for} \quad j_1 \neq j_2 \neq j_3 \quad (13) \\ \sqrt{\frac{1}{3}} & \text{for} \quad j_1 = j_2 \neq j_3 \quad (14) \\ \frac{1}{\sqrt{3}} \frac{2j_3+2}{2j_3+1} & \text{for} \quad j_1 \neq j_2,\ j_2 = j_3 \quad (15) \\ \frac{1}{\sqrt{3}} \frac{2j_3+3}{2j_3+1} & \text{for} \quad j_1 = j_2 = j_3, \quad (16) \end{cases}$$

and the matrix elements are

$$\langle^{A-4}\mathrm{Ni}, 2^+|T_{20}|^A\mathrm{Zn}, \text{g.s.}\rangle = F(j_1\, j_2\, j_3)\Lambda\sqrt{2}\lambda_{j_3}(-)^{l_1}\langle j_1||r^2Y_2||j_2\rangle(U_{j_1}V_{j_2}+U_{j_2}V_{j_1}) \times \left(\frac{U_{j_1}V_{j_2}}{E_{j_1}+E_{j_2}-\omega}+\frac{U_{j_1}V_{j_2}}{E_{j_1}+E_{j_2}+\omega}\right). \quad (17)$$

The factor Λ is the normalization constant in the RPA formulation; the term $\langle j_1||r^2Y_2||j_2\rangle$ is the matrix element of the quadrupole operator; the E_j are the quasiparticle energies and ω is the phonon energy which is assumed to be the empirical energy of the 2^+ state.

The parameters used throughout the calculations are the ones described in subsect. 4.1.4.

5. Results of the calculation

The G_{NL} factors corresponding to the different calculations are given in table 3. The BCS results have one extra value of $N = 7$ due to the fact that the $g_{\frac{9}{2}}$ level is also included in the calculation. Aside from this case the relative values for different N are in agreement in all the calculations.

The absolute value can be better discussed by studying the renormalization coefficient which has to be used in the program DWBA in order to fit the cross sections. This is given in table 2. The coefficients corresponding to the pure configuration case is much larger than the one used for the other calculations, reflecting the coherence of the residual interaction for the α-transfer processes.

The harmonic calculations predict a cross section for the ^{56}Fe(d, ^{6}Li)^{52}Cr about twice the value corresponding to ^{58}Ni(d, ^{6}Li)^{54}Fe, as it is suggested by the fact that the former is a transition between two-phonon states, while the second takes place between one-phonon states. In the pure configuration case, this ratio is somewhat smaller, due to Pauli corrections in the two-phonons states. However the shell model diagonalization predicts nearly the same cross sections, showing the existence of important anharmonicities in the pairing collective degree of freedom.

The ratio between the normalization constants for the Zn targets and the ^{58}Ni and ^{56}Fe targets is about 2.5 for the shell model diagonalization and about 7 for the harmonic case. Thus again the harmonic approximation overpredicts the increase in the cross section with the number of phonons. It is clear that Pauli corrections should play here an important role, since the neutrons are almost filling the f-p shell.

It is somewhat surprising that the BCS calculation should yield values of the cross sections which are about one-half of those corresponding to the shell model diagonalization. This may be at least partially explained by the fact that the ground state correlations in the $Z = 28$ case are neglected in our BCS approximations.

Finally, the renormalization D_0 values corresponding to the shell model diagonalization are such that it is not possible to use a constant D_0 for the five 0^+ transitions. The theoretical calculations predict that the cross sections for the Zn targets are

TABLE 3

The G_{NL} structure factors for the different models

	N	^{56}Fe	^{58}Ni	^{64}Zn	^{66}Zn	^{68}Zn
Shell model $0^+ \to 0^+$	0	0.0026	0.0028	0.0098	0.0097	0.0083
	1	0.0084	0.0085	0.0204	0.0200	0.0170
	2	0.0185	0.0156	0.0062	0.0064	0.0053
	3	0.0759	0.0687	0.0953	0.0919	0.0758
	4	0.169	0.153	0.224	0.214	0.176
	5	0.207	0.182	0.233	0.222	0.183
	6	0.199	0.189	0.398	0.370	0.299
Harmonic model $0^+ \to 0^+$	0	0.0027	0.0020	0.0115	0.0137	0.0160
	1	0.0089	0.0067	0.0243	0.0288	0.0333
	2	0.0192	0.0142	0.0088	0.0104	0.0118
	3	0.0779	0.0567	0.113	0.132	0.149
	4	0.177	0.128	0.272	0.313	0.350
	5	0.225	0.160	0.299	0.339	0.375
	6	0.216	0.151	0.480	0.539	0.590
Pure configurations $0^+ \to 0^+$	0	0.00024	0.00021			
	1	0.0013	0.0011			
	2	0.0016	0.0014			
	3	0.0016	0.0014			
	4	0.0225	0.0187			
	5	0.0670	0.0549			
	6	0.0568	0.0459			
BCS $0^+ \to 0^+$	0			0.0077	0.0074	0.0061
	1			0.0150	0.0144	0.0120
	2			0.00085	0.00062	0.0014
	3			0.0600	0.0593	0.0501
	4			0.149	0.144	0.120
	5			0.154	0.150	0.127
	6			0.309	0.282	0.226
	7			0.0077	0.0083	0.0082
Pure configurations $0^+ \to 2^+$	0	0.0010	0.00093			
	1	0.0018	0.0016			
	2	0.00096	0.00086			
	3	0.0165	0.0145			
	4	0.0561	0.0487			
	5	0.0507	0.0434			
BCS $0^+ \to 2^+$	0			0.0050	0.0050	0.0045
	1			−0.0021	−0.0012	−0.00044
	2			0.0137	0.0173	0.0190
	3			0.0472	0.0543	0.0559
	4			0.0515	0.0632	0.0683
	5			0.117	0.122	0.117
	6			0.0014	0.0018	0.0022

about twice those corresponding to the Ni zone, while the experimental results show cross sections of similar magnitude.

In ref. [5]) it is shown that when $T = 1$ and $T = 0$ pairing forces are present and when one of them is sufficiently strong so as to distort the corresponding field, changes in the other force do not modify sensibly the α-transfer cross section. It seems as if one of the forces is enough to saturate the cross sections.

The nuclei studied in this paper belong to the transitional region, as regard to the $T = 1$ force [4]), and the variations of the theoretical cross sections are a consequence of this fact. The similar magnitude of the empirical cross sections seems therefore to stem from the distortion induced by the $T = 0$ field, which was not taken into account in the present analysis.

The systematic underestimation of the $(2^+)/(0^+)$ ratio may be an indication of indirect processes being present. It is known that different channels are coupled stronger for excited 2^+ states than for 0^+ ground states.

References

1) A. E. Ceballos, H. J. Erramuspe, A. M. J. Ferrero, M. J. Sametband, J. E. Testoni, D. R. Bès and E. E. Maqueda, Nucl. Phys. **A208** (1973) 617
2) P. D. Kunz, University of Colorado, report COO-535-606, unpublished
3) G. G. Dussel, E. E. Maqueda and R. P. J. Perazzo, Nucl. Phys. **A153** (1970) 469
4) D. R. Bès, E. E. Maqueda and R. P. J. Perazzo, Nucl. Phys. **A199** (1973) 193
5) O. Dragún, G. G. Dussel, E. E. Maqueda and R. P. J. Perazzo, Nucl. Phys. **A167** (1971) 529
6) A. Bohr, Proc. Int. Symp. on nuclear structure, Dubna, 1968 (IAEA, Vienna, 1968) p. 179
7) G. G. Dussel, R. P. J. Perazzo, D. R. Bès and R. A. Broglia, Nucl. Phys. **A175** (1971) 513
8) B. Bayman, D. R. Bès and R. A. Broglia, Phys. Rev. Lett. **23** (1969) 1299
9) D. R. Bès, G. G. Dussel, E. E. Maqueda and R. P. J. Perazzo, Physica Scripta **6** (1972) 239
10) D. R. Bès, G. G. Dussel, E. E. Maqueda and R. P. J. Perazzo, Nucl. Phys., to be published
11) L. S. Kisslinger and R. Sorensen, Rev. Mod. Phys. **35** (1963) 910
12) D. R. Bès and R. Sorensen, Advances in nuclear physics, vol. 2 (Plenum Press, New York, 1969) p. 129